

Intensity correlations, entanglement properties and ghost imaging in multimode thermal-seeded parametric downconversion: Theory

Ivo P. Degiovanni,¹ Maria Bondani,² Emiliano Puddu,^{3,4} Alessandra Andreoni,^{3,4} and Matteo G. A. Paris^{5,6}

¹*Istituto Nazionale di Ricerca Metrologica, Torino, Italy*

²*National Laboratory for Ultrafast and Ultraintense Optical Science - C.N.R.-I.N.F.M., Como, Italy*

³*Dipartimento di Fisica e Matematica, Università degli Studi dell'Insubria, Como, Italia*

⁴*Consiglio Nazionale delle Ricerche, Istituto Nazionale per la Fisica della Materia (C.N.R.-I.N.F.M.), Como, Italia*

⁵*Dipartimento di Fisica, Università degli Studi di Milano, I-20133 Milano, Italia*

⁶*I.S.I. Foundation, I-10133 Torino, Italia*

(Dated: November 5, 2021)

We address parametric-downconversion seeded by multimode pseudo-thermal fields. We show that this process may be used to generate multimode pairwise correlated states with entanglement properties that can be tuned by controlling the seed intensities. Multimode pseudo-thermal fields seeded parametric-downconversion represents a novel source of correlated states, which allows one to explore the classical-quantum transition in pairwise correlations and to realize ghost imaging and ghost diffraction in regimes not yet explored by experiments.

I. INTRODUCTION

Ghost imaging [1] and ghost diffraction [2] consist in the retrieval of an object transmittance pattern or its Fourier transform, respectively by evaluating a fourth-order correlation function at the detection planes between the field that never interacted with the object and a correlated one transmitted by the object. A general ghost-imaging/diffraction scheme involves a source of correlated bipartite fields and two propagation arms usually called test (T) and reference (R). In the T-arm, where the object is placed, a bucket (or a point-like) detector measures the total light transmitted by it. The R-arm contains an optical setup suitable for reconstructing the image of the object or its Fourier transform and a position-sensitive detector [3].

The correlations needed for ghost imaging and ghost diffraction may be either quantum, as those shown by entangled states produced by spontaneous parametric downconversion (PDC) [1] or classical, as those present in the fields at the output of a beam-splitter fed with a pair of multi-mode pseudo-thermal beams [4, 5, 6]. In recent years several authors discussed analogies and differences between the two cases in terms of the achievable visibility and of the optical configurations needed for image reconstruction. An history of this debate from different point of views may be found in Refs. [3] and references therein. Recently, it has been suggested that the entangled nature of the light source [7, 8, 9] may be necessary to satisfy the “back-propagating” thin-lens equation, which, indeed, is fulfilled by PDC-based ghost imaging systems. Among other things, we prove that this claim is incorrect.

In this paper, we discuss the use of a novel, PDC-based, light source for ghost-imaging/diffraction. In our scheme (see Fig. 1), the nonlinear crystal realizing PDC is seeded by two multi-mode thermal (MMT) beams. We show that the entanglement properties and the amount of correlation at the output may be tuned by changing the intensities of the seeds, thus leading to a source that can be used to investigate the transition from the classical to the quantum regime. Besides, our

novel source allows ghost-image reconstruction with the same optical scheme used for ghost imaging based on spontaneous PDC, with the “back-propagating” thin-lens equation that is satisfied irrespective of the entanglement of the state. We notice that the effectiveness of the setup discussed here has been already demonstrated in the case of a crystal seeded with a single MMT beam [10].

The paper is structured as follows. In section II we calculate the state obtained from our PDC source with the injection of MMT seeds on both T- and R- arms, thus revealing that the output field on each arm maintains the statistics of the seed. In section III we analyze both the intensity correlations between the output beams and the entanglement properties of the overall state. We explicitly evaluate separability thresholds in terms of the seed intensities, and show that the condition for the existence of nonclassical correlations in intensity measurements subsumes the condition for inseparability, *i.e.* sub-shot-noise correlations are a sufficient condition for entanglement in our system. We also show that entanglement properties of the output field are not affected by losses taking place after the PDC interaction. In section IV we show that the state generated in our scheme satisfies the “back-propagating” thin-lens equation independently on the seed intensities, *i.e.* independently on being entangled or not, and it is suitable for realizing ghost-imaging and ghost diffraction experiments. Finally, Section V closes the paper with some concluding remarks.

II. PARAMETRIC DOWN-CONVERSION WITH THERMAL SEEDS

The interaction scheme we are going to consider is schematically depicted in Fig. 1. It consists in a nonlinear $\chi^{(2)}$ crystal pumped by a monochromatic non-depleted plane-wave propagating along the z -axis. The Hamiltonian describing the resulting parametric process is given by

$$H_I = \int d^2\mathbf{x} \int_0^L dz \chi^{(2)} E_p(\mathbf{x}, t) a_T(\mathbf{x}, t) a_R(\mathbf{x}, t) + h.c. \quad (1)$$

L being the crystal length and $\chi^{(2)}$ the nonlinear susceptibility. The pump-field may be written as $E_p(\mathbf{x}, t) = \mathcal{E}_p \exp[i(\Omega_p t - K_p z)]$ [11].

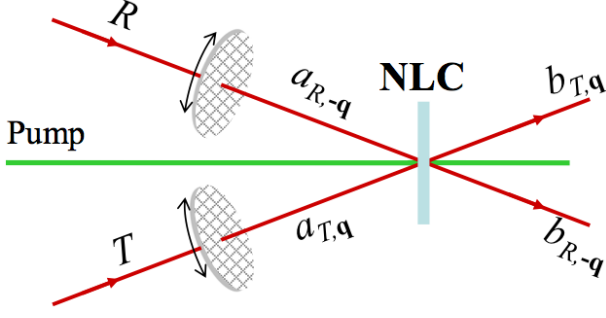


FIG. 1: Schematic diagram of the nonlinear interaction. T and R are the Test and Reference arms of the setup.

We can write the interacting quantum fields as

$$a_j(\mathbf{x}, t) \propto \sum_{\mathbf{q}, \nu_j} a_{j, \mathbf{q}, \nu_j} e^{i[K_{j,z} z + \mathbf{q}_j \cdot \mathbf{r} - (\Omega_j + \nu_j)t]} \quad (j = R, T) \quad (2)$$

where: $K_{j,z} = \sqrt{K_j^2 - \mathbf{q}_j^2}$, \mathbf{q}_j being the transverse momentum, $K_j = n_j(\Omega_j + \nu_j)/c$, n_j the index of refraction, Ω_j the selected central frequency in channel j , ν_j the frequency displacement with respect to Ω_j , and c is the speed of light in the vacuum. The commutation relation of the quantum fields are

$$\begin{aligned} [a_{j, \mathbf{q}, \nu}, a_{j', \mathbf{q}', \nu'}^\dagger] &= \delta_{j, j'} \delta_{\mathbf{q}, \mathbf{q}'} \delta_{\nu, \nu'} \quad (j, j' = R, T) \quad (3) \\ [a_{j, \mathbf{q}, \nu}, a_{j', \mathbf{q}', \nu'}] &= 0 \end{aligned}$$

The evolution of a quantum system induced by the interaction Hamiltonian (1) is described by the unitary operator $U = \exp(-i\hbar^{-1} \int H_I dt)$, where

$$-\frac{i}{\hbar} \int H_I dt = i \sum_{\mathbf{q}, \nu} \kappa_{\mathbf{q}, \nu} a_{T, \mathbf{q}, \nu} a_{R, -\mathbf{q}, -\nu} + h.c. \quad (4)$$

where $\kappa_{\mathbf{q}, \nu} \propto \text{sinc}[(K_p - K_{T,z} - K_{R,z})L/2]$. To obtain Eq. (4) we have exploited the conservation of energy at the central wavelength $\Omega_p = \Omega_T + \Omega_R$ obtaining $\nu_T = -\nu_R = \nu$, and the

conservation of transverse momentum $\mathbf{q}_T = -\mathbf{q}_R = \mathbf{q}$. As, according to Eq. (4), the extension to the non-monochromatic case is, in most of cases, straightforward, in the following analysis we will focus on the monochromatic emission at the frequencies Ω_R and Ω_T and hence we will drop the subscript ν from the variables.

The operator U can be rewritten in terms of the operators $S_{\mathbf{q}} = (\kappa_{\mathbf{q}} a_{T, \mathbf{q}} a_{R, -\mathbf{q}} + h.c.)$ as $U = \exp(i \sum_{\mathbf{q}} S_{\mathbf{q}})$. According to the commutation relations (3), we have $[S_{\mathbf{q}}, S_{\mathbf{q}'}] = 0$, and therefore $U = \bigotimes_{\mathbf{q}} e^{i S_{\mathbf{q}}}$, *i.e.* the interaction establishes pairwise correlations among the modes.

In our analysis we focus on the case in which both the T- and R-arms are seeded with MMT beams

$$\begin{aligned} \rho_{in} &= \bigotimes_{\mathbf{q}} \rho_{T, \mathbf{q}} \otimes \rho_{R, -\mathbf{q}} \quad (5) \\ \rho_{j, \mathbf{q}} &= \sum_{n=0}^{\infty} P_{j, \mathbf{q}}(n) |n\rangle_{j, \mathbf{q}} \langle n|, \end{aligned}$$

where $j = R, T$ and $|n\rangle_{j, \mathbf{q}}$ denotes the Fock number basis for the mode \mathbf{q} of the j -arm. The thermal profile of the input is given by

$$P_{j, \mathbf{q}}(n) = \mu_{j, \mathbf{q}}^n (1 + \mu_{j, \mathbf{q}})^{-n-1},$$

$\mu_{j, \mathbf{q}}$ being the average photon number per mode. The density matrix at the output is given by

$$\rho_{out} = U \rho_{in} U^\dagger = \bigotimes_{\mathbf{q}} e^{i S_{\mathbf{q}}} \rho_{T, \mathbf{q}} \otimes \rho_{R, -\mathbf{q}} e^{-i S_{\mathbf{q}}}, \quad (6)$$

According to [?], it is possible to “disentangle” $e^{i S_{\mathbf{q}}}$ by using the two-boson representation of the $SU(1,1)$ algebra as

$$\begin{aligned} e^{i S_{\mathbf{q}}} &= \exp\left\{\zeta_{\mathbf{q}} a_{T, \mathbf{q}}^\dagger a_{R, -\mathbf{q}}^\dagger\right\} \\ &\times \exp\left\{-\eta_{\mathbf{q}}(a_{T, \mathbf{q}}^\dagger a_{T, \mathbf{q}} + a_{R, -\mathbf{q}}^\dagger a_{R, -\mathbf{q}} + 1)\right\} \\ &\times \exp\left\{-\zeta_{\mathbf{q}}^* a_{T, \mathbf{q}} a_{R, -\mathbf{q}}\right\} \quad (7) \end{aligned}$$

where $\zeta_{\mathbf{q}} = -ie^{-i\varphi_{\mathbf{q}}} \tanh(|\kappa_{\mathbf{q}}|)$, $\eta_{\mathbf{q}} = \ln[\cosh |\kappa_{\mathbf{q}}|]$, and $e^{i\varphi_{\mathbf{q}}} = \kappa_{\mathbf{q}}/|\kappa_{\mathbf{q}}|$.

Equation (7) implies that

$$e^{i S_{\mathbf{q}}} |n\rangle_{T, \mathbf{q}} \otimes |m\rangle_{R, -\mathbf{q}} = \sum_{k=0}^{\min\{m, n\}} \sum_{l=0}^{\infty} C_{\mathbf{q}}(m, n, k, l) |n-k+l\rangle_{T, \mathbf{q}} \otimes |m-k+l\rangle_{R, -\mathbf{q}} \quad (8)$$

with

$$C_{\mathbf{q}}(m, n, k, l) = e^{-\eta_{\mathbf{q}}(n+m-2k+1)} \frac{\sqrt{n! m! (n-k+l)! (m-k+l)!}}{k! l! (n-k)! (m-k)!} \zeta_{\mathbf{q}}^l (-\zeta_{\mathbf{q}}^*)^k \quad (9)$$

By substituting Eq. (8) in Eq. (6), we obtain the output state

$$\rho_{out} = \bigotimes_{\mathbf{q}} \sum_{nm} P_{T,\mathbf{q}}(n) P_{R,-\mathbf{q}}(m) \sum_{k_1, k_2=0}^{\min\{m, n\}} \sum_{l_1, l_2=0}^{\infty} C_{\mathbf{q}}(m, n, k_1, l_1) C_{\mathbf{q}}(m, n, k_2, l_2)^* \times \\ |n - k_1 + l_1\rangle_{T,\mathbf{q}} \langle n - k_2 + l_2| \otimes |m - k_1 + l_1\rangle_{R,-\mathbf{q}} \langle m - k_2 + l_2| \quad (10)$$

As expected, the first moments of the photon distribution for each mode are those of a thermal statistics

$$\begin{aligned} \langle n_{T,\mathbf{q}} \rangle &= \text{Tr}(\rho_{out} a_{T,\mathbf{q}}^\dagger a_{T,\mathbf{q}}) = \mu_{T,\mathbf{q}} + n_{\text{PDC},\mathbf{q}}(1 + \mu_{T,\mathbf{q}} + \mu_{R,-\mathbf{q}}) \\ \langle n_{R,-\mathbf{q}} \rangle &= \text{Tr}(\rho_{out} a_{R,-\mathbf{q}}^\dagger a_{R,-\mathbf{q}}) = \mu_{R,-\mathbf{q}} + n_{\text{PDC},\mathbf{q}}(1 + \mu_{T,\mathbf{q}} + \mu_{R,-\mathbf{q}}) \\ \langle (\Delta n_{T,\mathbf{q}})^2 \rangle &= \langle n_{T,\mathbf{q}} \rangle (\langle n_{T,\mathbf{q}} \rangle + 1) \\ \langle (\Delta n_{R,-\mathbf{q}})^2 \rangle &= \langle n_{R,-\mathbf{q}} \rangle (\langle n_{R,-\mathbf{q}} \rangle + 1) \end{aligned} \quad (11)$$

where $\langle O \rangle = \text{Tr}[O \rho_{out}] = \text{Tr}[U^\dagger O U \rho_{in}]$, $\Delta O = O - \langle O \rangle$ and $n_{\text{PDC},\mathbf{q}} = \sinh^2 |\kappa_{\mathbf{q}}|$ is the average number of photons due to spontaneous PDC.

Notice that the case of vacuum inputs, $\rho_{in} = |0\rangle\langle 0|_T \otimes |0\rangle\langle 0|_R$, corresponds to spontaneous downconversion, *i.e.* to the generation of twin-beam, whereas the case of a single MMT on one arm and the vacuum on the other, $\rho_{in} = \bigotimes_{\mathbf{q}} (|0\rangle\langle 0|_{T,\mathbf{q}} \otimes \rho_{R,-\mathbf{q}})$ corresponds to the state considered in Ref. [10].

In the Heisenberg description, the modes after the interaction with the crystal are given by $b_{j,\mathbf{q}} = U^\dagger a_{j,\mathbf{q}} U$, *i.e.*

$$b_{j,\mathbf{q}} = \mathcal{U}_{\mathbf{q}} a_{j,\mathbf{q}} + e^{i\varphi_{\mathbf{q}}} \mathcal{V}_{\mathbf{q}} a_{j',-\mathbf{q}}^\dagger \quad (j, j' = R, T, j \neq j') \quad (12)$$

where $\mathcal{U}_{\mathbf{q}} = \cosh |\kappa_{\mathbf{q}}|$ and $\mathcal{V}_{\mathbf{q}} = \sinh |\kappa_{\mathbf{q}}|$ (and obviously $\mathcal{U}_{\mathbf{q}} = \mathcal{U}_{-\mathbf{q}}$, $\mathcal{V}_{\mathbf{q}} = \mathcal{V}_{-\mathbf{q}}$, and $\varphi_{\mathbf{q}} = \varphi_{-\mathbf{q}}$).

III. ENTANGLEMENT AND INTENSITY CORRELATIONS

In this section we address intensity correlations and entanglement properties of the beams generated in our scheme. As we will see, the amount of nonclassical correlations and entanglement may be tuned upon changing the intensity of the thermal seeds and there exist thresholds for the appearance of those nonclassical features. On the other hand, the index of total correlations (either classical or quantum) is a monotonically increasing function of the both the seed and the PDC energy.

A. Entanglement and separability

The downconversion process is known to provide pairwise entanglement between signal and idler beams. In our notations the (possibly) entangled mode are $a_{T,\mathbf{q}}$ and $a_{R,-\mathbf{q}}$. In the spontaneous process the output state is entangled for any value of the parametric gain (*i.e.* for any value of the crystal susceptibility, length ...) whereas in the case of a thermally seeded crystal the degree of entanglement crucially depends on the intensity of the seeds.

Since thermal states are Gaussian and the PDC Hamiltonian is bilinear in the field modes, the overall output state is also Gaussian. Therefore the entanglement properties may be evaluated by checking the positivity of the partial transpose (PPT condition), which represents a sufficient and necessary condition for separability for Gaussian pairwise mode entanglement [13]. Gaussian states are completely characterized by their covariance matrix. In this context let us introduce the “position”(-like) operators X and “momentum”(-like) operators Y

$$\begin{aligned} X_{j,\mathbf{q}} &= \frac{a_{j,\mathbf{q}} + a_{j,\mathbf{q}}^\dagger}{\sqrt{2}} \\ Y_{j,\mathbf{q}} &= \frac{a_{j,\mathbf{q}} - a_{j,\mathbf{q}}^\dagger}{i\sqrt{2}} \quad (j = R, T) \end{aligned} \quad (13)$$

Introducing the vector operator

$$\xi = (X_{T,\mathbf{q}_1}, Y_{T,\mathbf{q}_1}, X_{R,-\mathbf{q}_1}, Y_{R,-\mathbf{q}_1}, \dots)^T \quad (14)$$

with $m = 1, 2, \dots, \infty$, from the commutation relations (3) gives

$$[\xi_\alpha, \xi_\beta] = i\Omega_{\alpha,\beta} \quad (15)$$

where $\Omega = \bigoplus_m \omega \oplus \omega$ and ω is the symplectic matrix

$$\omega = \begin{pmatrix} 0 & 1 \\ -1 & 0 \end{pmatrix} \quad (16)$$

The covariance matrix V is calculated as $V_{\alpha,\beta} = 2^{-1} \langle \{\Delta \xi_\alpha, \Delta \xi_\beta\} \rangle$, where $\{O_1, O_2\}$ denotes the anti-commutator. Uncertainty relation among the position and momentum operators impose a constraint on the covariance matrix, $V + \frac{1}{2}\Omega \geq 0$, corresponding to the positivity of the state. The input-output relations for position and momentum operators are calculated according to Eq.s (12), obtaining

$$\begin{aligned} U^\dagger X_{j,\mathbf{q}} U &= \mathcal{U}_{\mathbf{q}} X_{j,\mathbf{q}} + \mathcal{V}_{\mathbf{q}} X_{j',-\mathbf{q}} \\ U^\dagger Y_{j,\mathbf{q}} U &= \mathcal{U}_{\mathbf{q}} Y_{j,\mathbf{q}} - \mathcal{V}_{\mathbf{q}} Y_{j',-\mathbf{q}} \quad (j, j' = R, T, j \neq j'). \end{aligned} \quad (17)$$

Without any loss of generality, in the derivation of Eq.s (17) we set $\varphi_{\mathbf{q}} = 0$ which, in turn, corresponds to a proper choice of the phase, or, equivalently to a proper redefinition of the operators $a_{j,\mathbf{q}}$ corresponding to a rotation of the phase space. From Eq.s (17) we calculate the covariance matrix

$$\mathbf{V} = \bigoplus_{m=1}^{\infty} \mathbf{V}_{\mathbf{q}_m} = \begin{pmatrix} \mathbf{V}_{\mathbf{q}_1} & \mathbf{0} & \mathbf{0} & \dots \\ \mathbf{0} & \mathbf{V}_{\mathbf{q}_2} & \mathbf{0} & \dots \\ \mathbf{0} & \mathbf{0} & \mathbf{V}_{\mathbf{q}_3} & \dots \\ \vdots & \vdots & \vdots & \ddots \end{pmatrix} \quad (18)$$

with

$$\mathbf{V}_{\mathbf{q}} = \begin{pmatrix} \mathcal{A}_{\mathbf{q}} & 0 & \mathcal{C}_{\mathbf{q}} & 0 \\ 0 & \mathcal{A}_{\mathbf{q}} & 0 & -\mathcal{C}_{\mathbf{q}} \\ \mathcal{C}_{\mathbf{q}} & 0 & \mathcal{B}_{\mathbf{q}} & 0 \\ 0 & -\mathcal{C}_{\mathbf{q}} & 0 & \mathcal{B}_{\mathbf{q}} \end{pmatrix} \quad (19)$$

where

$$\begin{aligned} \mathcal{A}_{\mathbf{q}} &= [\mathcal{U}_{\mathbf{q}}^2(2\mu_{T,\mathbf{q}} + 1) + \mathcal{V}_{\mathbf{q}}^2(2\mu_{R,-\mathbf{q}} + 1)]/2, \\ \mathcal{B}_{\mathbf{q}} &= [\mathcal{U}_{\mathbf{q}}^2(2\mu_{R,-\mathbf{q}} + 1) + \mathcal{V}_{\mathbf{q}}^2(2\mu_{T,\mathbf{q}} + 1)]/2, \\ \mathcal{C}_{\mathbf{q}} &= \mathcal{U}_{\mathbf{q}}\mathcal{V}_{\mathbf{q}}(\mu_{T,\mathbf{q}} + \mu_{R,-\mathbf{q}} + 1). \end{aligned} \quad (20)$$

\mathbf{V} satisfies the uncertainty relations ensuring the positivity of ρ_{out} .

In order to check whether and when the state ρ_{out} is entangled we apply the PPT criteria for Gaussian entanglement [13]. For instance, we apply the positive map $\mathcal{L}_{R,-\mathbf{q}'}$ to the state ρ_{out} . $\mathcal{L}_{R,-\mathbf{q}'}(\rho_{out})$ is the transposition (complex conjugation) only of the subspace $\mathcal{H}_{R,-\mathbf{q}'}$ corresponding to the mode $R,-\mathbf{q}'$. Simon showed that this corresponds to calculate the covariance matrix $\tilde{\mathbf{V}}$, where all the matrix-blocks $\mathbf{V}_{\mathbf{q}}$ remain the same excepts the matrix $\mathbf{V}_{\mathbf{q}'} \rightarrow \tilde{\mathbf{V}}_{\mathbf{q}'}$. $\tilde{\mathbf{V}}_{\mathbf{q}'}$ is calculated with a sign change in the $R,-\mathbf{q}'$ momentum variable ($Y_{R,-\mathbf{q}'} \rightarrow -Y_{R,-\mathbf{q}'}$), while the other momentum and position variables remain unchanged ($X_{T,\mathbf{q}'} \rightarrow X_{T,\mathbf{q}'}$, $Y_{T,\mathbf{q}'} \rightarrow Y_{T,\mathbf{q}'}$, and $X_{R,-\mathbf{q}'} \rightarrow X_{R,-\mathbf{q}'}$). Thus we obtain

$$\tilde{\mathbf{V}}_{\mathbf{q}'} = \begin{pmatrix} \mathcal{A}_{\mathbf{q}'} & 0 & \mathcal{C}_{\mathbf{q}'} & 0 \\ 0 & \mathcal{A}_{\mathbf{q}'} & 0 & \mathcal{C}_{\mathbf{q}'} \\ \mathcal{C}_{\mathbf{q}'} & 0 & \mathcal{B}_{\mathbf{q}'} & 0 \\ 0 & \mathcal{C}_{\mathbf{q}'} & 0 & \mathcal{B}_{\mathbf{q}'} \end{pmatrix}, \quad (21)$$

where $\mathcal{A}_{\mathbf{q}'}$, $\mathcal{B}_{\mathbf{q}'}$ and $\mathcal{C}_{\mathbf{q}'}$ are defined in Eq.s (20). According to PPT criteria, the separability of ρ_{out} , is guaranteed by the positivity of $\mathcal{L}_{R,-\mathbf{q}'}(\rho_{out})$, i.e.

$$\tilde{\mathbf{V}} + \frac{1}{2}\mathbf{\Omega} \geq 0. \quad (22)$$

Inequality (22) corresponds to

$$\mu_{T,\mathbf{q}'}\mu_{R,-\mathbf{q}'} - n_{\text{PDC},\mathbf{q}'}(1 + \mu_{T,\mathbf{q}'} + \mu_{R,-\mathbf{q}'}) \geq 0. \quad (23)$$

We observe that the spontaneous PDC corresponds to the situation with $\mu_{T,\mathbf{q}'} = \mu_{R,-\mathbf{q}'} = 0$, thus ρ_{out} is entangled. Also the case considered in Ref. [10], a MMT seeded PDC only on one arm (i.e., $\mu_{R,-\mathbf{q}'} = 0$) is always entangled. On the contrary, in the case of MMT seeded PDC on both arms, the

inequality (23) introduces a threshold. For instance, if we consider a MMT seed with the same mean number of photon per mode, μ , only when the inequality $\mu^2 \geq n_{\text{PDC},\mathbf{q}}(1 + 2\mu)$ is satisfied, ρ_{out} is separable. It is noteworthy to observe that if the PPT is applied to any other subspaces the inequality obtained are analogous to Eq. (23), and thus the result is the same.

B. Separability and losses

Her we address the problem of the effect of the losses on the separability of the state (10). In fact the presence of losses, e.g. internal reflection or absorption in the nonlinear crystal, may modify the quantum properties of the state, in particular the transition from entanglement to separability (in the absence of losses given by the Eq. (23)).

Losses in a quantum channel can be modeled by a beam splitter in one port of which the quantum channel is injected while the vacuum enters the other port. The model implies that Gaussian states after interaction are still Gaussian states due to the bi-linearity of the beam-splitter Hamiltonian. Thus also in the presence of losses, the covariance matrix completely describes the quantum state. If we consider an overall transmission factor τ on both channels we obtain the covariance matrix $\mathbf{V}_{\tau} = \tau\mathbf{V} + (1 - \tau)\mathbf{1}/2$. The form of the covariance matrix \mathbf{V}_{τ} is completely analogous to Eq. (18), where the block matrices $\mathbf{V}_{\mathbf{q}}$ are substituted with the block matrices $\mathbf{V}_{\tau,\mathbf{q}}$. $\mathbf{V}_{\tau,\mathbf{q}}$ has the same structure of $\mathbf{V}_{\mathbf{q}}$ in Eq. (19), where $\mathcal{A}_{\mathbf{q}}$, $\mathcal{B}_{\mathbf{q}}$, and $\mathcal{C}_{\mathbf{q}}$ are substituted by $\mathcal{A}_{\tau,\mathbf{q}} = \{1 + 2\tau[\mathcal{U}_{\mathbf{q}}^2\mu_{T,\mathbf{q}} + \mathcal{V}_{\mathbf{q}}^2(\mu_{R,-\mathbf{q}} + 1)]\}/2$, $\mathcal{B}_{\tau,\mathbf{q}} = \{1 + 2\tau[\mathcal{U}_{\mathbf{q}}^2\mu_{R,-\mathbf{q}} + \mathcal{V}_{\mathbf{q}}^2(\mu_{T,\mathbf{q}} + 1)]\}/2$, and $\mathcal{C}_{\tau,\mathbf{q}} = \tau\mathcal{C}_{\mathbf{q}}$, respectively. Thus, following the same line of thought of the previous section we obtain the covariance matrix $\tilde{\mathbf{V}}_{\tau}$, corresponding to the partial transposition of the state. According to PPT separability criteria, the state is separable if and only if the inequality $\tilde{\mathbf{V}}_{\tau} + \frac{1}{2}\mathbf{\Omega} \geq 0$ is fulfilled. This condition can be rewritten as

$$\tau^2[\mu_{T,\mathbf{q}'}\mu_{R,-\mathbf{q}'} - n_{\text{PDC},\mathbf{q}'}(1 + \mu_{T,\mathbf{q}'} + \mu_{R,-\mathbf{q}'})] \geq 0. \quad (24)$$

Since Ineq. (24) is fully equivalent to Ineq. (23), we conclude that losses do not affect the entanglement properties of the state in Eq. (10).

C. Intensity correlations

We now evaluate the pairwise intensity correlations owned by the generated beams. In addition, we analyze the connections between threshold for separability and the threshold required to have nonclassical correlations. As we will see a state obtained by thermally seeded PDC that exhibits sub shot-noise correlations is entangled, whereas the converse is not necessarily true. In other words, the existence of nonclassical intensity correlations is a sufficient condition for entanglement.

The normalized index of intensity correlation between a pair of modes $a_{j,\mathbf{q}}$ and $a_{j',\mathbf{q}'}$ is defined as

$$\gamma_{j,j'}(\mathbf{q}, \mathbf{q}') = \frac{\Gamma_{j,j'}(\mathbf{q}, \mathbf{q}')}{\sqrt{\langle(\Delta n_{T,\mathbf{q}})^2\rangle\langle(\Delta n_{R,-\mathbf{q}})^2\rangle}}. \quad (25)$$

where the correlation term is given by

$$\Gamma_{j,j'}(\mathbf{q}, \mathbf{q}') = \langle\Delta n_{j,\mathbf{q}}\Delta n_{j',\mathbf{q}'}\rangle. \quad (26)$$

Upon evaluating the first moments as we did in Eq. (11) we have, for the pair of modes $a_{T,\mathbf{q}}$ and $a_{R,-\mathbf{q}}$,

$$\begin{aligned} \Gamma_{T,R}(\mathbf{q}, -\mathbf{q}) &= n_{\text{PDC},\mathbf{q}}(1+n_{\text{PDC},\mathbf{q}})(1+\mu_{T,\mathbf{q}}+\mu_{R,-\mathbf{q}})^2 \\ &= \mathcal{C}_{\mathbf{q}}^2. \end{aligned} \quad (27)$$

A nonzero value of $\Gamma_{T,R}$, and hence of $\gamma_{T,R}$, indicates the presence of correlations between the considered modes. Perfect correlations correspond to $\gamma_{T,R} = 1$. Note that $\gamma_{T,R}$ is an increasing function of n_{PDC} , and does not undergo any threshold. In Fig 2 we plot $\gamma_{T,R}$ (solid lines) as a function of n_{PDC} in two different conditions, namely $\mu_T = 0$ and $\mu_R \neq 0$ (panel (a)) and $\mu_T = \mu_R \neq 0$ (panel (b)). As expected $\gamma_{T,R}$ approaches unit irrespectively of the mean values of the seeding thermal fields as soon as n_{PDC} becomes relevant. For large $n_{\text{PDC},\mathbf{q}}$ the index of correlation approaches unit as follows

$$\gamma_{T,R}(\mathbf{q}, -\mathbf{q}) \simeq 1 - \frac{1}{2} \frac{\mu_{T,\mathbf{q}} + \mu_{R,-\mathbf{q}} + 2\mu_{T,\mathbf{q}}\mu_{R,-\mathbf{q}}}{(1 + \mu_{T,\mathbf{q}} + \mu_{R,-\mathbf{q}})^2} \frac{1}{n_{\text{PDC},\mathbf{q}}^2}. \quad (28)$$

In the two cases $\mu_{T,\mathbf{q}} = \mu \gg 1$ and $\mu_{R,-\mathbf{q}} = 0$ (or viceversa) and $\mu_{T,\mathbf{q}} = \mu_{R,-\mathbf{q}} = \mu \gg 1$ we have, respectively

$$\begin{aligned} \gamma_{T,R}(\mathbf{q}, -\mathbf{q}) &\simeq 1 - \frac{1}{(1+n_{\text{PDC},\mathbf{q}})n_{\text{PDC},\mathbf{q}}} \frac{1}{2\mu} \\ \gamma_{T,R}(\mathbf{q}, -\mathbf{q}) &\simeq 1 - \frac{1}{(1+2n_{\text{PDC},\mathbf{q}})^2} + O\left(\frac{1}{\mu^2}\right). \end{aligned} \quad (29)$$

The nonclassical nature of this pairwise correlation may be assessed by the quantity [14]

$$NRF_{T,R}(\mathbf{q}) = \frac{\langle(\Delta n_{T,\mathbf{q}})^2\rangle + \langle(\Delta n_{R,-\mathbf{q}})^2\rangle - 2\Gamma_{T,R}(\mathbf{q}, -\mathbf{q})}{\langle n_{T,\mathbf{q}}\rangle + \langle n_{R,-\mathbf{q}}\rangle} \quad (30)$$

which is usually referred to as ‘‘the noise reduction factor’’. A noise reduction, $NRF_{T,R}(\mathbf{q}) < 1$, indicates the presence of nonclassical correlations. The value $NRF_{T,R}(\mathbf{q}) = 1$ is usually called ‘‘shot-noise limit’’ and corresponds to the case of a pair of uncorrelated coherent signals. By substituting the result for our system, we get

$$NRF_{T,R}(\mathbf{q}) = \frac{\mu_{T,\mathbf{q}}(1+\mu_{T,\mathbf{q}}) + \mu_{R,-\mathbf{q}}(1+\mu_{R,-\mathbf{q}})}{\mu_{T,\mathbf{q}} + \mu_{R,-\mathbf{q}} + 2n_{\text{PDC},\mathbf{q}}(1+\mu_{T,\mathbf{q}} + \mu_{R,-\mathbf{q}})} \quad (31)$$

We have $NRF_{T,R}(\mathbf{q}) < 1$ if

$$n_{\text{PDC},\mathbf{q}} > \frac{1}{2} \frac{\mu_{T,\mathbf{q}}^2 + \mu_{R,-\mathbf{q}}^2}{1 + \mu_{T,\mathbf{q}} + \mu_{R,-\mathbf{q}}}, \quad (32)$$

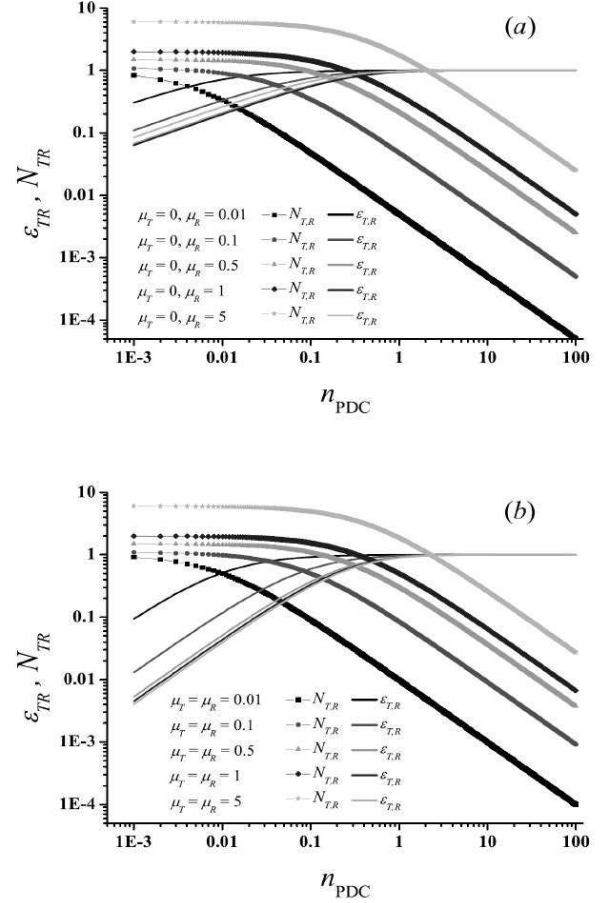


FIG. 2: The index of total correlations $\gamma_{T,R}$ (solid line) and the noise reduction factor $NRF_{T,R}$ (line plus symbol) as a function of n_{PDC} for the cases of (a): $\mu_T = 0$ and $\mu_R \neq 0$ and (b) $\mu_T = \mu_R \neq 0$. The values chosen for the parameters are indicated in the figures.

which subsumes the separability threshold of Eq. (23) and individuates the same region for $\mu_{T,\mathbf{q}} = \mu_{R,-\mathbf{q}}$. Therefore, for thermally seeded PDC, sub-shot noise correlations imply entanglement [15]. In Fig. 2 we also plot $NRF_{T,R}$ as a function of n_{PDC} for the same parameters used for $\gamma_{T,R}$. As expected, the figure shows that $NRF_{T,R}$ crosses the shot-noise level at different values of n_{PDC} that depend on the mean values of the thermal seeds, thus confirming the intuition that in order to achieve sub-shot noise correlations in the presence of two thermal seeds we need to have a PDC process strong enough.

IV. MMT-PDC BASED GHOST IMAGING AND GHOST DIFFRACTION

The bipartite state obtained by the nonlinear process described above is suitable for applications to ghost-imaging/diffraction protocols. Ghost-imaging and ghost diffraction protocols rely on the capability of retrieving an object transmittance pattern and its Fourier transform, respectively, by the evaluation of a fourth-order correlation function

at the detection planes of a light field that has never interacted with the object and a correlated one transmitted by the object. We consider the schemes depicted in Fig. 3. An object, described by the transmission function $t(\mathbf{x}_T')$, is inserted in the T-arm on the plane \mathbf{x}_T'' and a bucket detector measures the total light, I_T , transmitted by the transparency. The R-arm contains an optical setup suitable for reconstructing either the image of the object or its Fourier transform and a position-sensitive detector that measures the local $I_R(\mathbf{x}_R)$. The procedure for calculating the correlation function between the light detected in the two arms of the setup is equivalent to evaluating first the correlation function between $I_R(\mathbf{x}_R)$ and $I_T(\mathbf{x}_T)$:

$$G^{(2)}(\mathbf{x}_R, \mathbf{x}_T) = \langle \Delta I_R(\mathbf{x}_R) \Delta I_T(\mathbf{x}_T) \rangle, \quad (33)$$

and then integrating over all the values of \mathbf{x}_T

$$\mathcal{G}^{(2)}(\mathbf{x}_R) = \int d\mathbf{x}_T G^{(2)}(\mathbf{x}_R, \mathbf{x}_T), \quad (34)$$

where $\langle I_j(\mathbf{x}_i) \rangle = \langle c_j^\dagger(\mathbf{x}_j) c_j(\mathbf{x}_j) \rangle$ ($j = R, T$) is the mean intensity of the j -th beam at the detection plane, with hereinafter $\langle \dots \rangle = \text{Tr}(\dots \rho_{in})$, and $\langle I_R(\mathbf{x}_R) I_T(\mathbf{x}_T) \rangle = \langle c_R^\dagger(\mathbf{x}_R) c_R(\mathbf{x}_R) c_T^\dagger(\mathbf{x}_T) c_T(\mathbf{x}_T) \rangle$.

The connection between the field operators at the detection planes and those at the output of the crystal is given by

$$c_j(\mathbf{x}_i) = \int d\mathbf{x}'_j h_j(\mathbf{x}_j, \mathbf{x}'_j) b_j(\mathbf{x}'_j), \quad (35)$$

where $b_j(\mathbf{x}'_j)$ are the Reference and Test field operators at the output face of the crystal and $h_R(\mathbf{x}_R, \mathbf{x}'_R)$ and $h_T(\mathbf{x}_T, \mathbf{x}'_T)$ are the two response functions describing the propagation of the field in the two arms of the setup [16].

By using Eqs. (35) and (34) we can rewrite $G^{(2)}(\mathbf{x}_R, \mathbf{x}_T)$ as

$$G^{(2)}(\mathbf{x}_R, \mathbf{x}_T) = \int d\mathbf{x}'_R d\mathbf{x}''_R d\mathbf{x}'_T d\mathbf{x}''_T h_R(\mathbf{x}_R, \mathbf{x}'_R) h_R^*(\mathbf{x}_R, \mathbf{x}''_R) h_T(\mathbf{x}_T, \mathbf{x}'_T) h_T^*(\mathbf{x}_T, \mathbf{x}''_T) \times \left[\langle b_R^\dagger(\mathbf{x}''_R) b_R(\mathbf{x}'_R) b_T^\dagger(\mathbf{x}''_T) b_T(\mathbf{x}'_T) \rangle - \langle b_R^\dagger(\mathbf{x}''_R) b_R(\mathbf{x}'_R) \rangle \langle b_T^\dagger(\mathbf{x}''_T) b_T(\mathbf{x}'_T) \rangle \right] \quad (36)$$

Also in this case the factorization rule for $\langle b_R^\dagger(\mathbf{x}''_R) b_R(\mathbf{x}'_R) b_T^\dagger(\mathbf{x}''_T) b_T(\mathbf{x}'_T) \rangle$ is the same as that for spontaneous PDC [17], and for multi-thermal one-arm-seeded PDC [10]

$$\langle b_R^\dagger(\mathbf{x}''_R) b_R(\mathbf{x}'_R) b_T^\dagger(\mathbf{x}''_T) b_T(\mathbf{x}'_T) \rangle = \langle b_R^\dagger(\mathbf{x}''_R) b_R(\mathbf{x}'_R) \rangle \langle b_T^\dagger(\mathbf{x}''_T) b_T(\mathbf{x}'_T) \rangle + \langle b_R^\dagger(\mathbf{x}''_R) b_T^\dagger(\mathbf{x}''_T) \rangle \langle b_R(\mathbf{x}'_R) b_T(\mathbf{x}'_T) \rangle. \quad (37)$$

The result in Eq. (37) can be demonstrated by rewriting $b_j(\mathbf{x})$ in terms plane waves as $b_j(\mathbf{x}) \propto \sum_{\mathbf{q}} e^{i\mathbf{q}\cdot\mathbf{x}} b_{j,\mathbf{q}}$ and then exploiting the input-output relation of Eq. (12). According to Eq. (37), and in complete analogy with the case of spontaneous PDC [17], also in the case of the MMT-seeded PDC we obtain

$$G^{(2)}(\mathbf{x}_R, \mathbf{x}_T) = \left| \int d\mathbf{x}'_R \int d\mathbf{x}'_T h_R(\mathbf{x}_R, \mathbf{x}'_R) h_T(\mathbf{x}_T, \mathbf{x}'_T) \langle b_R(\mathbf{x}'_R) b_T(\mathbf{x}'_T) \rangle \right|^2 \quad (38)$$

where

$$\langle b_R(\mathbf{x}'_R) b_T(\mathbf{x}'_T) \rangle \propto \sum_{\mathbf{q}} e^{i[\mathbf{q}\cdot(\mathbf{x}'_T - \mathbf{x}'_R) + \varphi_{\mathbf{q}}]} \mathcal{U}_{\mathbf{q}} \mathcal{V}_{\mathbf{q}} (1 + \mu_{T,\mathbf{q}} + \mu_{R,-\mathbf{q}}) = \sum_{\mathbf{q}} e^{i[\mathbf{q}\cdot(\mathbf{x}'_T - \mathbf{x}'_R) + \varphi_{\mathbf{q}}]} \mathcal{C}_{\mathbf{q}}. \quad (39)$$

and $\mathcal{C}_{\mathbf{q}}$ is calculated in Eq. (20) By using Eq. (39), Eq. (38) can be rewritten as

$$G^{(2)}(\mathbf{x}_R, \mathbf{x}_T) = \left| \sum_{\mathbf{q}} \tilde{h}_R(\mathbf{x}_R, -\mathbf{q}) \tilde{h}_T(\mathbf{x}_T, \mathbf{q}) \mathcal{C}_{\mathbf{q}} \right|^2 \quad (40)$$

where $\tilde{h}_j(\mathbf{x}_j, \mathbf{q}) = \int d\mathbf{x}'_j e^{i\mathbf{q}\cdot\mathbf{x}'_j} h_j(\mathbf{x}_j, \mathbf{x}'_j)$.

According to Fig. 3, we consider two different schemes for the collection optics in the Test arm of the setup:

(a) the detection plane coincides with the plane of the transparency, $\mathbf{x}_T' = \mathbf{x}_T$, and hence

$$\tilde{h}_T(\mathbf{x}_T, \mathbf{q}) \propto e^{-i\frac{\lambda d_1}{4\pi} q^2} e^{-i\mathbf{q}\cdot\mathbf{x}_T} t(\mathbf{x}_T) \quad (41)$$

only describes free propagation over a distance d_1 ;

(b) a collection lens is located on the plane $\mathbf{x}_{l,T}$ beyond the transparency in a Fourier-transform configuration, and hence

$$\tilde{h}_T(\mathbf{x}_T, \mathbf{q}) \propto e^{-i\frac{\lambda d_1}{4\pi} q^2} \tilde{t}(-\mathbf{q} - \frac{2\pi}{\lambda f_T} \mathbf{x}_T). \quad (42)$$

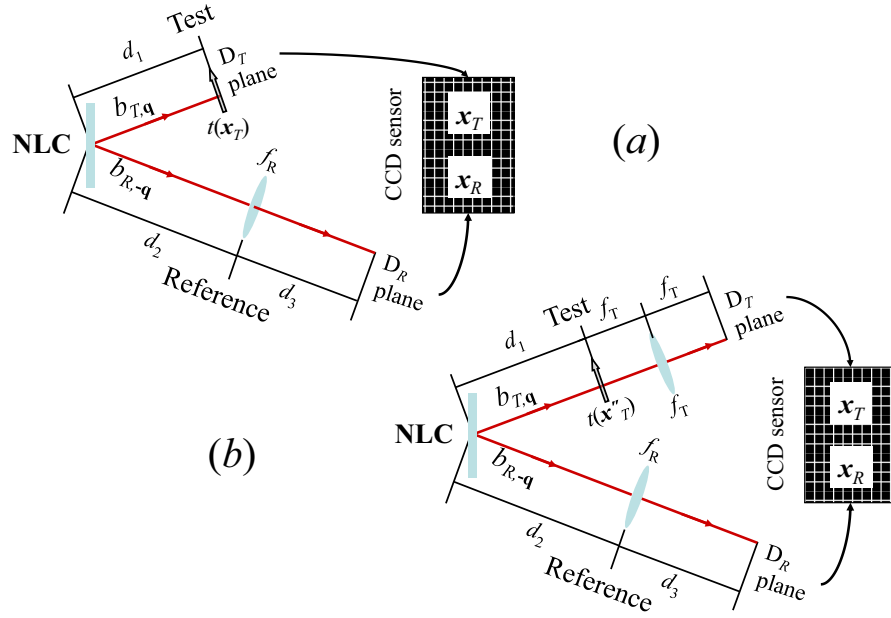


FIG. 3: Experimental setup for ghost imaging: $t(\mathbf{x}_T)$, object transmission function; $f_{T,R}$. (Left): experimental configuration with detection plane coinciding with the object plane. (Right): experimental configuration with detection plane coinciding with the Fourier plane of the collecting lens in the Test arm.

The optical scheme in the Reference arm contains a lens (focal length f_R) located at $\mathbf{x}_{l,R}$ and thus the Fourier transform of the impulse response functions can be written as

$$\begin{aligned} \tilde{h}_R(\mathbf{x}_R, -\mathbf{q}) &\propto \int d\mathbf{x}'_R e^{-i\mathbf{q}\cdot\mathbf{x}'_R} \int d\mathbf{x}_{l,R} e^{i\frac{\pi}{\lambda d_2}(\mathbf{x}_{l,R}-\mathbf{x}'_R)^2} e^{-i\frac{\pi}{\lambda f_R}\mathbf{x}_{l,R}^2} e^{i\frac{\pi}{\lambda d_3}(\mathbf{x}_{l,R}-\mathbf{x}_R)^2} \\ &\propto e^{-i\frac{\lambda d_2}{4\pi}q^2} \int d\mathbf{x}_{l,R} e^{-i\left(\frac{2\pi}{\lambda d_3}\mathbf{x}_R+\mathbf{q}\right)\cdot\mathbf{x}_{l,R}} e^{i\frac{\pi}{\lambda}\left(\frac{1}{d_3}-\frac{1}{f_R}\right)\mathbf{x}_{l,R}^2}. \end{aligned} \quad (43)$$

If $f_R \neq d_3$, Eq. (43) becomes

$$\tilde{h}_R(\mathbf{x}_R, -\mathbf{q}) \propto e^{-i\frac{\lambda}{4\pi}\left(d_2+\frac{1}{1/d_3-1/f_R}\right)q^2} e^{-\frac{i}{d_3}\frac{1}{1/d_3-1/f_R}\mathbf{q}\cdot\mathbf{x}_R}, \quad (44)$$

while if $f_R = d_3$, Eq. (43) becomes

$$\tilde{h}_R(\mathbf{x}_R, -\mathbf{q}) \propto e^{-i\frac{\lambda d_2}{4\pi}q^2} \delta\left(\frac{2\pi}{\lambda d_3}\mathbf{x}_R+\mathbf{q}\right). \quad (45)$$

Depending on the chosen geometrical configuration, these schemes realize either a ghost-imaging or a ghost-diffraction experiment [18].

A. Ghost imaging

To perform a ghost-imaging experiment we choose $f_R \neq d_3$. Let us first consider case (a). Substituting Eq. (41) and Eq. (44) into Eq. (40) yields the expression

$$\begin{aligned} G^{(2)}(\mathbf{x}_R, \mathbf{x}_T) &\propto |t(\mathbf{x}_T)|^2 \left| \sum_{\mathbf{q}} \mathcal{C}_{\mathbf{q}} e^{-i\mathbf{q}\cdot\left(\mathbf{x}_T+\frac{1}{d_3}\frac{1}{1/d_3-1/f_R}\mathbf{x}_R\right)} e^{-i\frac{\lambda}{2\pi}\frac{d_1+d_2}{1/d_3-1/f_R}\left(\frac{1}{d_1+d_2}+\frac{1}{d_3}-\frac{1}{f_R}\right)q^2} \right|^2 \\ &\simeq |t(\mathbf{x}_T)|^2 |\mathcal{C}_{\mathbf{q}}|^2 \delta\left(\mathbf{x}_T+\frac{\mathbf{x}_R}{M}\right), \end{aligned} \quad (46)$$

which, once integrated over the bucket detector,

$$G^{(2)}(\mathbf{x}_R) = \int d\mathbf{x}_T G^{(2)}(\mathbf{x}_R, \mathbf{x}_T) \simeq \left| t\left(-\frac{\mathbf{x}_R}{M}\right) \right|^2 |\mathcal{C}_{\mathbf{q}}|^2, \quad (47)$$

gives the image of the object. Note that in passing from Eq. (40) to Eq. (47) we have made the following assumptions: $\mathcal{C}_{\mathbf{q}}$ is almost independent of \mathbf{q} and the distances d_1 , d_2 and d_3 satisfy the so-called “back-propagating thin lens equation”, $1/(d_1 + d_2) + 1/d_3 = 1/f_R$ [19], so that we obtain an imaging system with magnification factor $M = d_3/(d_1 + d_2)$. In case (b), that is with a collection lens in the Test arm we proceed similarly by substituting Eq. (42) and Eq. (44) into Eq. (40) and making the same assumptions as before:

$$\begin{aligned} G^{(2)}(\mathbf{x}_R, \mathbf{x}_T) &\propto \left| \sum_{\mathbf{q}} \mathcal{C}_{\mathbf{q}} \tilde{t}\left(-\mathbf{q} - \frac{2\pi}{\lambda f_T}\right) e^{-i\frac{1}{d_3} \frac{1}{1/d_3 - 1/f_R} \mathbf{q} \cdot \mathbf{x}_R} e^{-i\frac{\lambda}{2\pi} \frac{d_1+d_2}{1/d_3 - 1/f_R} \left(\frac{1}{d_1+d_2} + \frac{1}{d_3} - \frac{1}{f_R}\right) q^2} \right|^2 \\ &\simeq \left| t\left(-\frac{\mathbf{x}_R}{M}\right) \right|^2 |\mathcal{C}_{\mathbf{q}}|^2 . \end{aligned} \quad (48)$$

Note that in this case (b) the image of the object emerges from correlations without need to perform the integration over the bucket detector in order to recover the ghost image.

B. Ghost diffraction

To perform a ghost-diffraction experiment we consider the configuration $d_3 = f_R$ and choose configuration (b) in the Test arm. By inserting Eq. (42) and Eq. (45) into Eq. (40)

$$\begin{aligned} G^{(2)}(\mathbf{x}_R, \mathbf{x}_T) &\propto \left| \sum_{\mathbf{q}} \mathcal{C}_{\mathbf{q}} \tilde{t}\left(-\mathbf{q} - \frac{2\pi}{\lambda f_T}\right) e^{-i\frac{\lambda}{4\pi}(d_1+d_2)q^2} \delta\left(\frac{2\pi}{\lambda d_3} \mathbf{x}_R - \mathbf{q}\right) \right|^2 \\ &\simeq \left| \tilde{t}\left(-\frac{2\pi}{\lambda d_3} \mathbf{x}_R - \frac{2\pi}{\lambda f_T} \mathbf{x}_T\right) \right|^2 |\mathcal{C}_{\mathbf{q}}|^2 . \end{aligned} \quad (49)$$

By selecting the component $\mathbf{x}_T = 0$ on the Test plane we get

$$G^{(2)}(\mathbf{x}_R, 0) \simeq \left| \tilde{t}\left(-\frac{2\pi}{\lambda d_3} \mathbf{x}_R\right) \right|^2 |\mathcal{C}_{\mathbf{q}}|^2 , \quad (50)$$

which gives the diffraction pattern of the object. Note that the choice (a) would not give any meaningful result.

V. CONCLUSIONS AND OUTLOOKS

This paper was aimed at showing the possibility of performing ghost imaging and ghost diffraction with a novel source based on PDC seeded with two MMT fields, which generates a bipartite correlated state. Peculiar properties of this new source may open a new insight into the understanding of the ghost imaging/diffraction process. In fact, nowadays the sources considered for ghost imaging/diffraction either were definitely separable (classically correlated beams obtained from a MMT source) or entangled (spontaneous PDC). On the contrary, here we proved that the separable/entangled nature of the light produced by our source can be controlled by changing the seed intensities and that the transition from quantum to classical regimes does not modify the possibility of realizing ghost imaging schemes.

Furthermore, we also showed that a ghost imaging experiment performed with our source satisfies the “back-propagating” thin-lens equation, as much as with spontaneous

PDC, even when the state produced becomes separable. This is in contrast with the idea, also recently suggested [7, 8, 9], that the “back-propagating” thin-lens equation is connected with the entangled nature of the spontaneous PDC.

According to the consideration of above, we are planning to realize a ghost imaging experiment with a MMT seeded PDC source in order to show that the same optical configuration allows retrieving of the image irrespectively to the entangle or separable nature of the light produced by the source. This will definitely demonstrate that there is not any connection between the entangled properties of the light source and the “back-propagating” thin-lens equation.

Acknowledgments

This work has been supported by MIUR project PRIN2005024254-002.

[1] T. B. Pittman, *et al.*, Phys. Rev. A **52**, R3429 (1995).

[2] D.V. Strekalov, *et al.*, Phys.Rev.Lett. **74**, 3600 (1995),

- P.H.Souto Ribeiro, *et al.*, Phys.Rev.A **49**, 4176 (1994).
- [3] M. D'Angelo and Y. H. Shih, Laser Phys. Lett. **2**, 567 (2005), A. Gatti *et al.*, J. Modern Opt. **53**, 736 (2006), Y. Shih, arXiv:0707.0268 (2007); A. Gatti et al, Phys. Rev. Lett. **98**, 039301 (2007).
- [4] A. Valencia *et al.*, Phys. Rev. Lett. **94**, 063601 (2005).
- [5] D. Zhang *et al.*, Opt. Lett. **30**, 2354 (2005).
- [6] F. Ferri *et al.*, Phys. Rev. Lett. **94**, 183602 (2005).
- [7] De-Zhong Cao *et al.*, Phys. Rev. A **71**, 013801 (2005).
- [8] Y. Cai, et al., Opt. Lett. **29**, 2716 (2004).
- [9] Y. Cai, et al., Phys. Rev. E **71**, 056607 (2005).
- [10] E. Puddu, *et al.*, Opt. Lett. **32**, 1132 (2007); for the generalization to multiple parametric processes see e.g. A. Ferraro et al, J. Opt. Soc. Am. B **21**, 1241 (2004); A. Allevi et al., Opt. Lett. **29**, 180 (2004).
- [11] L. Mandel and E. Wolf, *Optical Coherence and Quantum Optics* (Cambridge University Press, 1995)
- [12] D. Traux, Phys Rev. D. **31**, 1988, (1985).
- [13] R. Simon, Phys. Rev. Lett, **84**, 2726, (2000).
- [14] A. Agliati et al, J. Opt. B, **7**, 652 (2005).
- [15] M. Bondani et al, quant-ph/0612198, Phys. Rev. A, in press.
- [16] J. W. Goodman, *Fourier Optics* (McGraw-Hill, New York, 1968).
- [17] E. Brambilla, A. Gatti, M. Bache, and L. A. Lugiato, Phys. Rev. A **69**, 023802 (2004), A. Gatti, E. Brambilla, M. Bache, and L. A. Lugiato, Phys. Rev. Lett. **93** (2004) 093602, A. Gatti, E. Brambilla, M. Bache, and L. A. Lugiato, Phys. Rev. A **70** (2004) 013802.
- [18] A. Gatti *et al.* Phys. Rev. Lett. **90**, 133603 (2003), J. C. Howell *et al.* Phys. Rev. Lett. **92**, 210403 (2004), M. D'angelo *et al.* Phys. Rev. Lett. **92**, 233601 (2004).
- [19] A. F. Abouraddy, B. E. A. Saleh, A. V. Sergienko, and M. C. Teich, J. Opt. Soc. Am. **19** 1177 (2002).